GEOLOGICA CARPATHICA, AUGUST 2020, 71, 4, 382–387 https://doi.org/10.31577/GeolCarp.71.4.6

Short Communication

$^{40}Ar/^{39}Ar$ step-heating dating of phlogopite and kaersutite megacrysts from the Železná hůrka (Eisenbühl) Pleistocene scoria cone, Czech Republic

LUKÁŠ KRMÍČEK[1,2,✉], MARTIN J. TIMMERMAN[3], MARTIN A. ZIEMANN[3], MASAFUMI SUDO[3] and JAROMÍR ULRYCH[1]

[1]Institute of Geology of the Czech Academy of Sciences, Rozvojová 269, CZ-165 02 Prague 6, Czech Republic; ✉lukas.krmicek@gmail.com
[2]Brno University of Technology, Faculty of Civil Engineering, AdMaS Centre, Veveří 95, CZ-602 00 Brno, Czech Republic
[3]Institut für Geowissenschaften, Universität Potsdam, Karl-Liebknecht-Straße 24–25, Haus 27, D-14476 Potsdam-Golm, Germany

(Manuscript received February 25, 2020; accepted in revised form May 6, 2020; Associate Editor: Igor Broska)

Abstract: $^{40}Ar/^{39}Ar$ step-heating of mica and amphibole megacrysts from hauyne-bearing olivine melilitite scoria/tephra from the Železná hůrka yielded a 435±108 ka isotope correlation age for phlogopite and a more imprecise 1.55 Ma total gas age of the kaersutite megacryst. The amphibole megacrysts may constitute the first, and the younger phlogopite megacrysts the later phase of mafic, hydrous melilitic magma crystallization. It cannot be ruled out that the amphibole megacrysts are petrogenetically unrelated to tephra and phlogopite megacrysts and were derived from mantle xenoliths or disaggregated older, deep crustal pegmatites. This is in line both with the rarity of amphibole at Železná hůrka and with the observed signs of magmatic resorption at the edges of amphibole crystals.

Keywords: Bohemian Massif, Železná hůrka, Eisenbühl, argon dating, mica, amphibole, melilitite.

Introduction

Stretching of Variscan crust in the north-western Bohemian Massif started in the Late Cretaceous and ultimately resulted in the formation of the Ohře/Eger Rift (OR). The OR represents the easternmost part of the European Cenozoic Rift System (Ziegler 1994) (Fig. 1A). Extension-related and mantle-derived alkaline volcanism started at ca. 80 Ma, peaked in the Eocene to Miocene (42–16 Ma) and lasted until 300,000 years ago (Ulrych et al. 2011 and references therein). The Cheb Basin (CB) is superimposed at the junction of the OR with the Cheb–Domažlice Graben (CHDG) (Kopecký 1986). The CHDG represents a NW–SE trending asymmetrical structure limited by the nearly 100 km-long Mariánské Lázně Fault (MLF) forming the eastern boundary and the Aš–Tachov Fault (ATF) forming the western boundary (Fig. 1B).

Pleistocene volcanic eruptions in western Bohemia form a volcanic field producing mafic, volcanic products of small volume, forming cinder cones such as those at Železná hůrka (Eisenbühl) and Komorní hůrka (Kammerbühl) (KH, ZH in Fig. 1B). They originated from lithospheric mantle characterized by $^{206}Pb/^{204}Pb$ ratios below 19.4 that was substantially modified via interaction with convective mantle (Krmíčková et al. 2020). Based on results of exploration trenching (Geissler et al. 2004) and coring with attendant gravity and magnetic studies (Mrlina et al. 2007, 2009), the presence of a Quaternary maar (Mýtina maar, M in Fig. 1B) was proven. It is situated ca. 300 m NW of the Železná hůrka cinder cone. An additional Pleistocene maar was discovered ESE of Neualbenreuth in Germany, ca. 2.5 km south of Železná hůrka (NA in Fig. 1B; Rohrmüller et al. 2017) and two other Pleistocene maars ca. 10 km NW of Komorní hůrka (Hošek et al. 2019; ZR and B in Fig. 1B). The cinder-cones and maars are aligned along, the ATF (ATF, Fig. 1B).

K–Ar ages for scoria from Železná hůrka range between 430 ka and 1.0 Ma (Šibrava & Havlíček 1980; Lustrino & Wilson 2007) and 110 ka and 2.0 Ma for lava from Komorní hůrka (Šibrava & Havlíček 1980; Todt & Lippolt 1975). An older 5 Ma age was obtained for tuff from a volcano south of the Mýtina village (ca. 1 km north of Železná hůrka and ca. 1 km NNE of the Mýtina maar).

Anomalously old K–Ar ages of the host rocks of the megacrysts result from incorporation of excess argon into the parent melt by heat-induced degassing of old, potassium-rich (thus ^{40}Ar rich) country rocks (e.g., Esser et al. 1997). Presence of xenoliths of the Variscan phyllites in the volcanic bomb of hauyne-bearing olivine melilitite from Mýtina (17 Ma) has been published by Ulrych et al. (2013).

Mica from the later volcanic rocks of the Železná hůrka cone shows a younger, 300±60 ka alpha-recoil age (Gögen & Wagner 2000). Wagner et al. (2002) reported a 365 ka fission track mean age for apatite from a hornblendite xenolith from volcaniclastic rocks near Mýtina. $^{40}Ar/^{39}Ar$ step-heating and *in situ* laser ablation dating of phlogopite megacrysts recovered from the trench west of the Mýtina village yielded 288±17 Ka age average (Mrlina et al. 2007). In contrast, step-heating

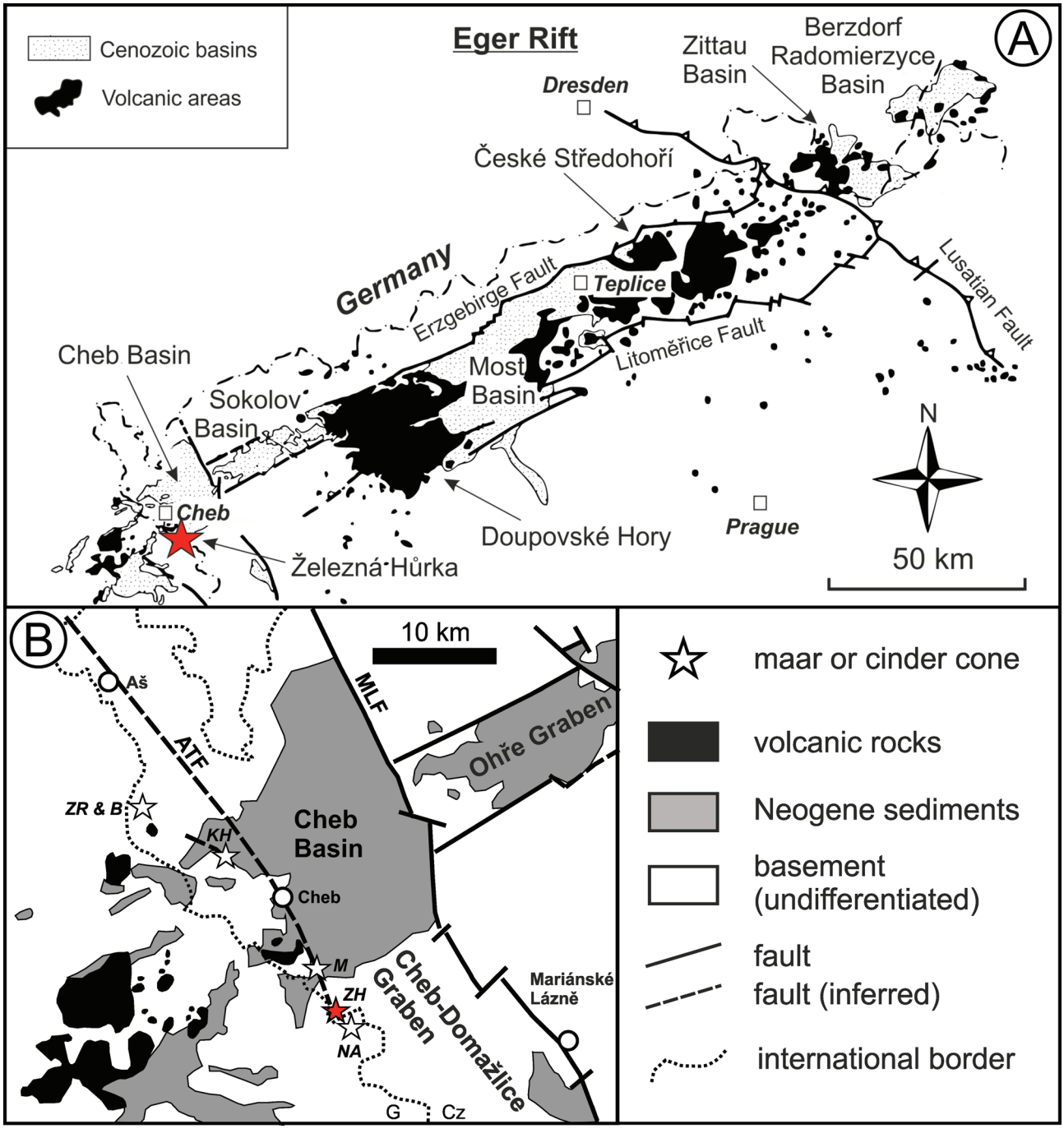

Fig. 1. A — Simplified geological map of the Ohře Rift showing Cenozoic sedimentary and volcanic rocks, main faults, Cheb Basin and the location of the Železná hůrka cone (modified from Kopecký 1986 and Ulrych et al. 2011). **B** — Simplified geological map of the Cheb Basin showing basement (undifferentiated), Neogene sediments, volcanic rocks, young volcanic centres and faults (modified from Mrlina et al. 2007). Abbreviations: KH=Komorní hůrka, M=Mýtina, NA=Neualbenreuth, ZH=Železná hůrka, ZR & B=Ztracený rybník and Bažina, ATF=Aš–Tachov Fault, MLF=Mariánské Lázně Fault.

dating of groundmass of an olivine nephelinite rock fragment from the tephra yielded a much older 1.57±0.36 Ma plateau age (Mrlina et al. 2007).

Generally, K–Ar and $^{40}Ar/^{39}Ar$ dating of young Cenozoic mafic rocks, may be problematic due to their low age (low radiogenic ^{40}Ar content), presence of xenoliths, and deleterious effects of alteration. The combined effects often result in widely varying groundmass K–Ar ages with large analytical uncertainties, and in anomalously young ages due to alteration-related ^{40}Ar loss. In contrast, anomalously old ages may result from incorporation of excess argon into the (ultra)mafic parent melt by heat-induced degassing of old, potassium-rich (thus ^{40}Ar rich) country rocks.

We carried out $^{40}Ar/^{39}Ar$ step-heating dating on a phlogopite and a kaersutite megacryst from the Železná hůrka (49°59'29.5"N, 12°26'39.7"E) with the aim of obtaining better radiometric age constraints for the young volcanic activity in the Cheb area and comparing these with ages obtained by other dating methods.

The Železná hůrka volcano

Situated at the junction of two prominent Cenozoic structures, namely the OR and the superimposed CHDG, Western Bohemia is probably one of the most seismically unstable zones of the Bohemian Massif. The CB is situated precisely at the junction of these two structures, with the MLF forming a topographic feature at the eastern limit of the CHDG (MLF, Fig. 1B) (Kopecký 1986). Nevertheless, Pleistocene melilitic magmatic rocks occur exclusively near the western limit of the CB, in the vicinity of a fault belonging to the ATF (ATF, Fig. 1B).

The Železná hůrka cinder cone is composed of scoriaceous hauyne-bearing olivine melilitite (Ulrych et al. 2013; Skála et al. 2015). Hradecký (1994) recognized three, 2.5 to 8 m thick sequences composed of ca. 10 scoria beds that are overlain unconformably by a welded coarse-grained spatter deposit. Grain-size analysis by Hradecký (1994) indicates that the lower, first stage of the volcanic sequence was formed by the Strombolian type activity that gradually passed into the Hawaiian-type fountains producing welded spatter. The lowermost sequence of the Hawaiian welded spatter deposits contains bedded material of the Strombolian tuffs (Hradecký 1994). The two eruption types were not necessarily separated by a long-lasting hiatus. Brandl et al. (2015) recognized three eruptive units: a basal unit of phreatomagmatic volcaniclastic material (lapilli sized tephra with fresh and glassy interiors), overlain by a highly olivine-phyric, unaltered blocky lava in the former vent (corresponding to Hradecký's (1994) welded spatter) containing abundant juvenile and lithic xenoliths and up to centimetre-sized crystals of olivine, clinopyroxene and phlogopite, in turn overlain by up to 5–7 m thick tephra layers with abundant xenoliths of basement crystalline rocks at the top.

Sample preparation and analytical methods

Several megacrysts were collected at the Železná hůrka area, namely, from a former quarry set in the Železná hůrka cinder cone, and from its foreland, maximally up to ca. 200 m to the north in the direction of Mýtina. From this collection, two megacrysts were selected for $^{40}Ar/^{39}Ar$ step-heating dating: a kaersutite (Eb-1) megacryst and a phlogopite (Eb-2) megacryst, both sampled directly from the Hawaiian spatter deposit (Hradecký 1994) exposed in the lower part of the north face of the Železná hůrka (see Supplementary Fig. S1).

Amphibole Eb-1 was carefully crushed by hand using a small steel mortar and piston and the fragments sieved to obtain the 250–500 micron grain size fraction. The grains were washed with lukewarm water with a few drops of chlorine-free detergent, followed by washing in acetone and dried in an oven at ca. 50 °C. Subsequently, the amphibole grains were leached for ca. 10 minutes in a few millilitres of 1M HNO_3 in an ultrasonic bath to remove carbonates that may be present, and leached for ca. 10 minutes at room temperature in ca. 7 % HF in an ultrasonic bath. This will remove any surface mineral contaminants and destroy most alteration products in microcracks. After rinsing and drying at ca. 50 °C, the sample was sieved to remove fines that may have formed due to disaggregation of grains, and the best grains were then handpicked under a binocular reflected light microscope with up to 40 times magnification. The phlogopite crystal Eb-2 was split into thin, clean fragments using a razor blade and small, ca. 2×2 mm and ca. 0.5 mm thick fragments cut using sharp scissors. Note that the phlogopite was not leached.

The grain samples were individually wrapped in commercial-grade aluminium foil and thus packed into a sample container made of 99.999 % pure Al. The sample container was wrapped in 0.5 mm thick cadmium foil and irradiated for 96 hours in position 6 of the FRG-1 facility of the GKSS research centre at Geesthacht (GeNF, Germany) in September 2006. The neutron flux variation of the length of the sample container was monitored by FC3 Fish Canyon Tuff sanidine, which was prepared by the Geological Survey of Japan (Uto et al. 1997). J values at the location of unknown samples were obtained by their interpolation. For correction for interfering Ar isotopes derived from Ca and K in the samples, crystals of CaF_2 and K_2SO_4 were irradiated together with the samples.

The $^{40}Ar/^{39}Ar$ analyses were carried out at the argon geochronology laboratory of the University of Potsdam, which uses a Gantry Dual Wave laser system with a 50 W CO_2 laser (wavelength 10.6 micrometre) for gas extraction. The gas is purified in an ultra-high vacuum line using SAES getters (one at 400 °C and one at room temperature) and a stainless steel finger cold trap that was cooled to the freezing point of ethanol (−114 °C), and analysed using a Micromass 5400 noble gas mass spectrometer with a high sensitivity and an ultra-low background. The mass spectrometer is fitted with an electron multiplier pulse counting system suitable for analysing small amounts of argon.

The gas fractions were extracted by heating the mineral grains with a 2000 micrometre diameter, defocused continuous laser beam for a few seconds to 1 minute, and cleaned for 10 minutes in the purification line before being let into the mass-spectrometer. Blanks were run at the start of each session and after every three unknowns.

The analytical data were corrected for background contributions, mass discrimination (using the composition of atmospheric argon), interference and the decay of the neutron-induced nuclides produced during irradiation following Uto et al. (1997). The $^{40}Ar/^{39}Ar$ ages were calculated using the 27.5 Ma age of FC3 (Ishizuka 1998), atmospheric $^{40}Ar/^{36}Ar$ ratio, 295.5, and decay constants from Steiger &

Jäger (1977). The average interference correction values are: $(^{36}Ar/^{37}Ar)_{Ca}=(4.222\pm0.03)\times10^{-4}$, $(^{39}Ar/^{37}Ar)_{Ca}=(9.025\pm0.023)\times10^{-4}$, $(^{38}Ar/^{39}Ar)_{K}=(1.721\pm0.026)\times10^{-2}$, and $(^{40}Ar/^{39}Ar)_{K}=(68.71\pm10.99)\times10^{-4}$.

The ratio of net intensities of each Ar isotope against the intensities of the blank for the temperature steps with fractions of ^{39}Ar in the total ^{39}Ar amount are more than 3 % were in the following ranges; ^{40}Ar: 134–4, ^{39}Ar: 20922–968, ^{38}Ar: 18913–55, ^{37}Ar: 675–0.2 and ^{36}Ar: 82–3. The age data were calculated and plotted following Uto et al. (1997).

All the uncertainties on the ages for total-gas ages and in age spectra, isotope correlation plots and in Supplementary Table S1 include the uncertainty in the irradiation parameter J (0.4 %) and are reported on the 1σ level. The uncertainty of the J value is estimated at 0.4 % as the conservative random error at each location in sample containers, and derived from all J values (ca. 200 analyses) obtained from the first four irradiations carried out by us at the GeNF reactor.

In addition, $^{40}Ar/^{39}Ar$ ages were calculated using the 28.294 Ma age for FC3 in combination with the newly proposed decay constants for ^{40}K (Renne et al. 2010, 2011). The atmospheric Ar isotope ratios of 298.56 for $^{40}Ar/^{36}Ar$ (Lee et al. 2006) were used. The data are available on request from the corresponding author. $^{40}Ar/^{39}Ar$ incremental step-heating data for the analysed phlogopite and kaersutite are available in Supplementary Table S1.

Results

Phlogopite megacryst Eb-2 yielded a 631±53 ka (1 sigma) plateau age for 8 gas fractions comprising 91 % of the ^{39}Ar released (Fig. 2A). The inverse isotope correlation age for the plateau-defining gas fractions is somewhat younger at 435±108 ka with an $^{40}Ar/^{36}Ar$ intercept ratio of 305±5, slightly higher than that of air ($^{40}Ar/^{36}Ar=295.5$, see above; Fig. 2B).

In contrast, step-heating dating of amphibole megacryst Eb-1 did not yield a plateau age due to the release of an unexpectedly large amount of Ar (48 % of the ^{39}Ar released) during fusion at the highest experimental temperature (Fig. 2C). The total gas age is 1.55±0.02 Ma and a 1.53±0.02 Ma weighted-mean age can be calculated for 7 gas fractions that have very similar apparent ages and comprise 39 % of the ^{39}Ar released. Although these gas fractions do not define a plateau as they comprise <50 % of the total ^{39}Ar released, a 1.42±0.08 Ma inverse isotope correlation age and $^{40}Ar/^{36}Ar$ intercept ratio of 318±19 were calculated for comparative purposes (Fig. 2D). However, the 1.54±0.02 Ma apparent age of the last and largest gas fraction (48 % of the ^{39}Ar released), the total gas age, weighted-mean and inverse isotope correlation ages (for 7 steps, including the last) all agree with each other within 2 sigma uncertainty. For this reason, we prefer the 1.55 Ma total gas age as the most plausible age for the amphibole megacryst.

For comparison purposes and future reference we also report the ages calculated using the 28.294 Ma age for monitor FC3 of Renne et al. (2010, 2011) and the atmospheric Ar isotope ratios of Lee et al. (2006). The plateau and inverse isotope correlation ages phlogopite megacryst Eb-2 are, respectively, 649±55 ka and 446±112 ka with an $^{40}Ar/^{36}Ar$ intercept ratio of 309±5. The total gas and weighted-mean correlation ages for amphibole megacryst Eb-1 are, respectively, 1.59±0.02 Ma and 1.57±0.02 Ma. The inverse isotope correlation age is 1.69±0.03 Ma with a $^{40}Ar/^{36}Ar$ intercept ratio of 284±6.

Discussion

Note that for plateau age calculations it is assumed that all non-radiogenic argon in the sample is atmospheric, but that for calculation of isotope correlation ages no assumptions are made about the nature of the trapped non-radiogenic argon component(s). The 435±108 ka age of phlogopite is equivalent within 2-sigma level to the 288±17 ka phlogopite $^{40}Ar/^{39}Ar$ age average reported for the tephra/tuffs exposed west of Mýtina village by Mrlina et al. (2007), and with the nominal pre 357 ka age of deposition of the oldest cored lake sediments in the Mýtina maar.

The ca. 1.55 Ma age of the kaersutite megacryst from the Železná hůrka cone is similar to the ca. 1.57 Ma age reported by Mrlina et al. (2007) for an olivine nephelinite from the tephra west of Mýtina village. Furthermore, Kämpf et al. (1993) described a kaersutite inclusion in an olivine megacryst – phenocryst from the Železná hůrka cone, showing that at least some of the amphiboles must have crystallized early. Forsterite contents of olivine phenocrysts in scoriaceous hauyne-bearing olivine melilitite from Železná hůrka vary between Fo_{86} and Fo_{90} (Brandl et al. 2015), indicating that they are high pressure cognate phenocrysts that crystallized at upper mantle depths. Such observations suggest that the kaersutite megacrysts are not simply fragments of an older, deeper pegmatitic intrusion (i.e. xenocrysts) but may be petrogenetically related to the volcanic rocks making up the Železná hůrka cone. On the other hand, it cannot be ruled out that the amphiboles are petrogenetically unrelated to the tephra and phlogopite megacrysts and were derived from mantle xenoliths or disaggregated older, deep crustal pegmatites. Indicators may be the rarity of amphiboles at Železná hůrka and the evidence for their magmatic partial resorption.

A two-phase origin of amphibole and clinopyroxene phenocrysts in volcanic rocks may have resulted in the presence of antecrysts that did not crystallize directly from the magma as represented by the host rock, but crystallized as phenocrysts in a discrete but kindred magmatic precursor (Hildreth & Wilson 2007). Such antecrysts probably are recycled mineral phases that formed during an earlier stage of the same magma plumbing system (Jerram & Martin 2008). Their cores crystallized in thinned lithosphere beneath the OR at a depth of ca. 25 km (Ulrych et al. 2018), in a magma chamber that received repeated injections of a hydrous magma that mixed with the residual magma, causing the evolved crystallization of

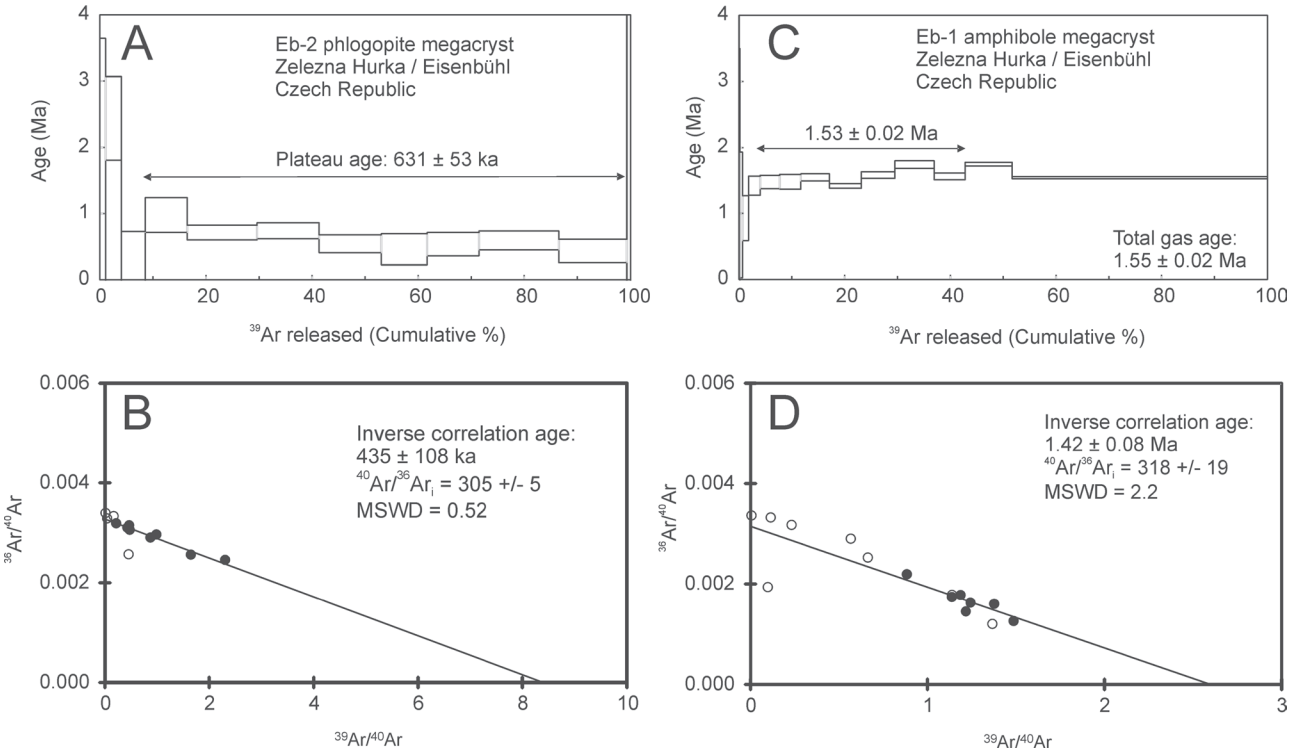

Fig. 2. $^{39}Ar/^{40}Ar$ step-heating spectra for phlogopite (**A**) and kaersutite megacrysts (**C**) with corresponding inverse isotope correlation ages (**B** resp. **D**). The arrows mark the gas fractions that were used in the plateau, weighted-mean and isotope correlation calculations.

the mafic macrocrysts. Hence, phlogopite macrocrysts are likely to be products of the late hydrous magma. Furthermore, the approximately 1 Ma older age of the amphibole from Železná hůrka points to earlier fractionation at deep crustal levels of the mafic parent melt that also produced the younger phlogopite megacrysts (Mg# 89) during an advanced stage of fractionation.

Conclusions

The 435±108 ka Ar–Ar isotope correlation age for phlogopite from the Železná hůrka cinder-cone overlaps within 2-sigma level the 288±17 ka phlogopite $^{40}Ar/^{39}Ar$ age average of the tephra (Mrlina et al. 2007), and also agrees with the stratigraphic evidence from the sediment fill of Mýtina maar.

The older 1.55 Ma age of the kaersutite megacryst puts an older age limit on the volcanic activity at Železná hůrka. Its presence is explained by an at least two-stage fractionation history of the Železná hůrka parent melt during which kaersutite megacrysts constitute the first, and the younger phlogopite megacrysts the later products of a mafic hydrous magma. Nevertheless, it cannot be excluded that kaersutite megacrysts resulted as antecrysts that crystallized as a discrete but kindred magmatic precursor or they represent upper mantle cognate inclusions or disrupted fragments of cumulates from mafic magma.

Acknowledgements: This research was financially supported (JU, LK) by the Research Plan RVO 67985831 of the Institute of Geology of the CAS, as well as by the BUT project LO1408 "AdMaS UP – Advanced Materials, Structures and Technologies", supported by the Ministry of Education, Youth and Sports under the "National Sustainability Programme I". The authors greatly appreciate Petr Martinec (Institute of Geonics of the Czech Academy of Sciences) and Jaroslav Lexa (Earth Science Institute, Slovak Academy of Sciences) for their reviews and valuable comments on the manuscript and handling editor Igor Broska for perfect editorial work.

References

Brandl P.A., Genske F.S., Beier C., Haase K.M., Sprung P. & Krumm S.H. 2015: Magmatic evidence for carbonate metasomatism in the lithospheric mantle underneath the Ohře (Eger) Rift. *J. Petrol.* 56, 1743–1774. https://doi.org/10.1093/petrology/egv052

Esser R.P., McIntosh W.C., Heizler M.T. & Kyle P.R. 1997: Excess argon in melt inclusions in zero-age anorthoclase feldspar from Mt. Erebus, Antarctica, as revealed by the $^{40}Ar/^{39}Ar$ method. *Geochim. Cosmochim. Acta* 18, 3789-3801. https://doi.org/10.1016/S0016-7037(97)00287-1

Geissler W.H., Kämpf H., Bankwitz P. & Bankwitz E. 2004: Das quartäre Tephra-Tuff-Vorkommen von Mytina (Südrand des westlichen Eger-Grabens/Tschechische Republik): Indikationen für Ausbruchs-und Deformationsprozesse. *Z. geol. Wiss.* 32, 31–54.

Gögen K. & Wagner G.A. 2000: Alpha-recoil track dating of Quaternary volcanics. *Chem. Geol.* 166, 127–137. https://doi.org/10.1016/S0009-2541(99)00185-0

Hildreth W. & Wilson C.J.N. 2007: Compositional zoning of the Bishop Tuff. *J. Petrol.* 48, 951–999. https://doi.org/10.1093/petrology/egm007

Hošek J., Valenta J., Rapprich V., Hroch T., Turjaková V., Tábořík P. & Pokorný P. 2019: Newly identified Pleistocene maars in Western Bohemia (Czech Republic) [Nově identifikované pleistocenní maary v západních Čechách]. *Geosci. Res. Rep.* 52, 197–104 (in Czech with English abstract). https://doi.org/10.3140/zpravy.geol.2019.23

Hradecký P. 1994: Volcanology of Železná and Komorní hůrka in Western Bohemia. *Věst.Čes. Geol. Úst.* 69, 89–92.

Ishizuka O. 1998: Vertical and horizontal variation of fast neutron flux in a single irradiation capsule and their significance in the laser-heating $^{40}Ar/^{39}Ar$ analysis: case study for the hydraulic rabbit facility of the JMTR reactor, Japan. *Geochem. J.* 32, 243–252. https://doi.org/10.2343/geochemj.32.243

Jerram D.A. & Martin. V.M. 2008: Understanding crystal populations and their significance through the magma plumbing system. In: Annen C. & Zellmer G.F. (Eds.): Dynamics of Crustal Magma Transfer, Storage and Differentiation. *Geol. Soc. London, Spec. Publ.* 304, 33–148. https://doi.org/10.1144/SP304.7

Kämpf H., Seifert W. & Ziemann M., 1993: Mantel-Kruste-Wechselwirkung im Bereich der Marienbader Störungszone. Teil 1: Neue Ergebnisse zum quartären Vulkanismus in NW-Böhmen. *Z. geol. Wiss.* 21,117–134.

Kopecký L. 1986: Geological development and block structure of the Cenozoic Ohře Rift (Czechoslovakia). In: Proc. 6th Intern. Conf. Bas. Tect. Salt Lake City, 114–124.

Krmíčková S., Krmíček L., Romer R.L. & Ulrych J. 2020: Lead isotope evolution of the Central European upper mantle: Constraints from the Bohemian Massif. *Geoscience Frontiers* 11, 3, 925–942. https://doi.org/10.1016/j.gsf.2019.09.009

Lee J-Y., Mart K., Severinghaus J.P., Kawamura K., Yoo H-S., Lee J.B. & Kim J.S. 2006: A redetermination of the isotopic abundances of atmospheric Ar. *Geochim. Cosmochim. Acta* 70, 4507–4512. https://doi.org/10.1016/j.gca.2006.06.1563

Lustrino M. & Wilson M. 2007: The circum-Mediterranean anorogenic Cenozoic igneous province. *Earth-Science Reviews* 81, 1–85. https://doi.org/10.1016/j.earscirev.2006.09.002

Mrlina J., Kämpf H., Geissler W.H. & van den Bogaard P. 2007: Assumed Quaternary maar structure at the Czech/German boundary between Mýtina and Neualbentreuth (western Eger Rift, Central Europe): geophysical, petrochemical and geochronological indications. *Z. geol. Wiss.* 35, 213–230.

Mrlina J., Kämpf H., Kroner C., Mingram J., Stebich M., Brauer A., Geissler W.H., Kallmeyer J., Matthes H. & Seidl M. 2009: Discovery of the first Quaternary maar in the Bohemian Massif, Central Europe, based on combined geophysical and geological surveys. *J. Volcanol. Geotherm. Res.* 182, 97–112. https://doi.org/10.1016/j.jvolgeores.2009.01.027

Renne P.R., Mundil R., Balco G., Min K. & Ludwig K.R. 2010: Joint determination of ^{40}K decay constants and $^{40}Ar^*/^{40}K$ for the Fish Canyon sanidine standard, and improved accuracy for $^{40}Ar/^{39}Ar$ geochronology. *Geochim. Cosmochim.* Acta 74, 5349–5367. https://doi.org/10.1016/j.gca.2010.06.017

Renne P.R., Mundil R., Balco G., Min K. & Ludwig K.R. 2011: Response to the comment by W.H. Schwarz et al. on "Joint determination of ^{40}K decay constants and $^{40}Ar^*/^{40}K$ for the Fish Canyon sanidine standard, and improved accuracy for $^{40}Ar/^{39}Ar$ geochronology" by P.R. Renne et al. (2010). *Geochim. Cosmochim. Acta* 75, 5097–5100. https://doi.org/10.1016/j.gca.2011.06.021

Rohrmüller J., Kämpf H., Geiß E., Großmann J., Grun I., Mingram J., Mrlina J., Plessen B., Stebich M., Veress C., Wendt A. & Nowaczyk N. 2017: Reconnaissance study of an inferred Quaternary maar structure in the western part of the Bohemian Massif near Neualbenreuth, NE-Bavaria (Germany). *Int. J. Earth Sci.* 107, 1381–1405. https://doi.org/10.1007/s00531-017-1543-0

Skála R., Ulrych J. Krmíček L., Fediuk F, Ackerman L. & Balogh K. 2015: Upper Cretaceous to Pleistocene melilitic volcanic rocks of the Bohemian Massif: petrology and mineral chemistry. *Geol. Carpath.* 66, 197–216. https://doi.org/10.1515/geoca-2015-0020

Steiger R.H. & Jäger E. 1977: Subcommission on geochronology: Convention on the use of decay constants in geo- and cosmochronology. *Earth Planet. Sci. Lett.* 36, 359–362.

Šibrava V. & Havlíček P. 1980: Radiometric age of Plio–Pleistocene volcanic rocks of the Bohemian Massif. *Věst.Ústř. Úst. Geol.* 55, 129–139.

Todt W. & Lippolt H.J. 1975: K–Ar Altersbestimmungenan Vulkaniten bekannter paläomagnetischer Feldrichtung. I. Oberpfalz und Oberfranken. *J. Geophys.* 41, 43–61.

Ulrych J., Dostal J., Adamovič J., Jelínek E., Špaček P. Hegner E. & Balogh K. 2011: Recurrent Cenozoic volcanic activity in the Bohemian Massif (Czech Republic). *Lithos* 123, 133–144. https://doi.org/10.1016/j.lithos.2010.12.008

Ulrych J., Ackerman L., Balogh K., Hegner E., Jelínek E., Pécskay Z., Přichystal A., Upton B.G.J., Zimák J. & Foltýnová R. 2013: Plio–Pleistocene basanitic and melilititic series of the Bohemian Massif: K–Ar ages, major/trace element and Sr–Nd isotopic data. *Chem. Erde* 73, 429–450. https://doi.org/10.1016/j.chemer.2013.02.001

Ulrych J., Krmíček L., Teschner C., Skála R., Adamovič J., Ďurišová J., Křížová Š., Kubošková S. & Radoň M. 2018: Chemistry and Sr-Nd isotope signature of amphiboles of the magnesio-hastingsite–pargasite–kaersutite series in Cenozoic volcanic rocks: Insight into lithospheric mantle beneath the Bohemian Massif. *Lithos* 312–313, 308–321. https://doi.org/10.1016/j.lithos.2018.05.017

Uto K., Ishizuka O., Matsumoto A., Kamioka H. & Togashi S. 1997: Laser-heating $^{40}Ar/^{39}Ar$ dating system of the Geological Survey of Japan: system outline and preliminary results. *Bull. Geol. Surv. Japan* 48, 23–46.

Wagner G.A., Gögen K., Jonckheere R., Wagner I. & Woda C. 2002: Dating of the Quaternary volcanoes Komorni Hurka (Kammerbühl) and Zelezna Hurka (Eisenbühl), Czech Republic, by TL, ESR, alpha-recoil and fission track chronometry. *Z. geol. Wiss.* 3, 191–200.

Ziegler P.A. 1994: Cenozoic rift system of Western and Central Europe: an overview. *Geol. Mijnbouw* 73, 99–127.

Supplement

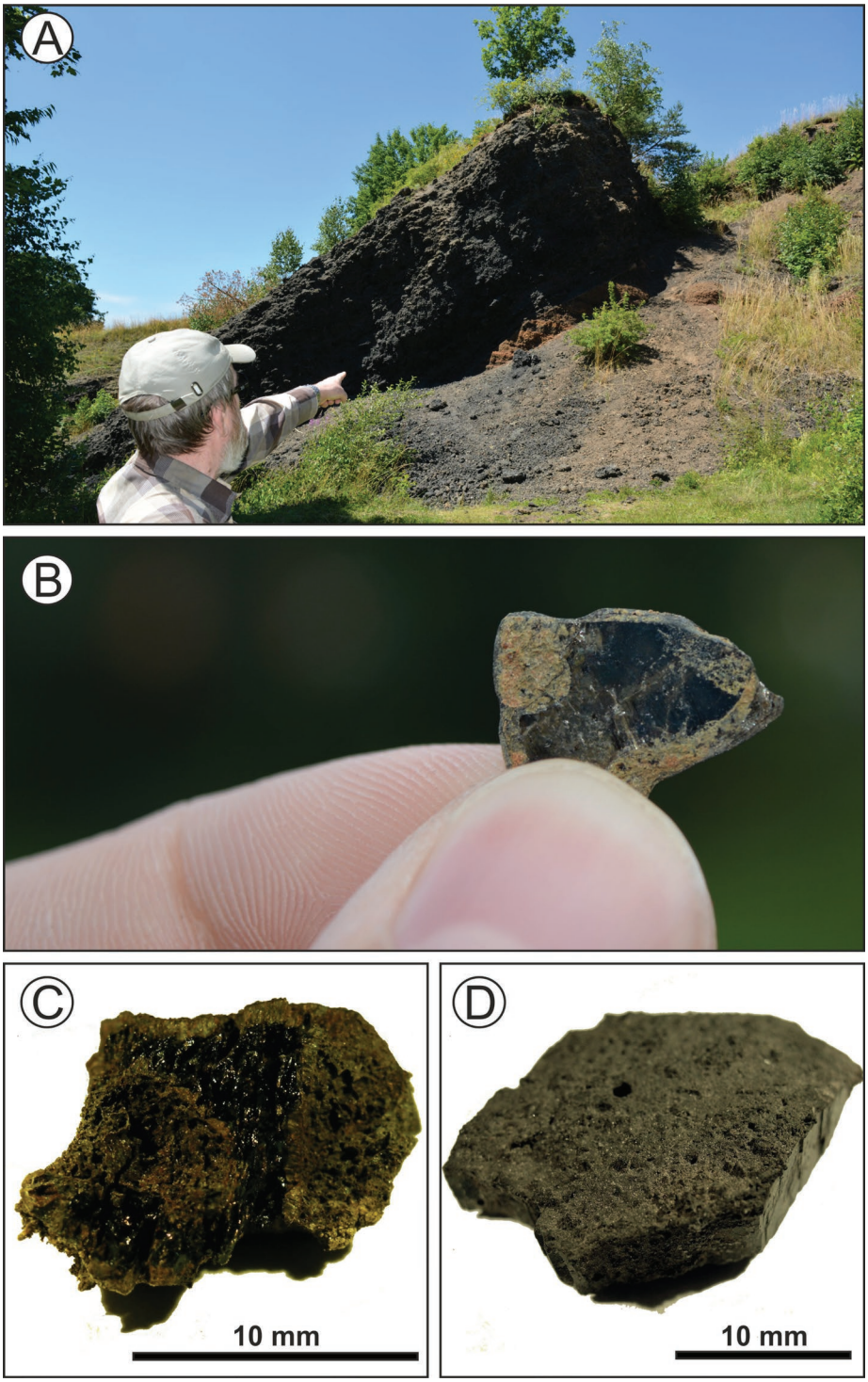

Fig. S1. A — North side of exposed cinder cone at Železná hůrka with prominent, dark coloured, welded Hawaiian spatter deposit (left) overlying an older phase of bedded Strombolian scoria (right). Bedding is visible in orange coloured rocks below the contact (centre). **B** — A phlogopite megacryst from Železná hůrka. **C** and **D** — Cinder-coated amphibole megacrysts from the tephra deposits immediately north of the Železná hůrka cone. The amphibole shown in C is partly corroded; D shows the 120° cleavage angle of amphibole.

Table S1: $^{40}Ar/^{39}Ar$ incremental step-heating data for phlogopite Eb-2 and amphibole Eb-1 from the Železná hůrka scoria cone, Cheb Basin, Czech Republic. Analytical uncertainties are presented at 1-s level. t.f.=total fusion.

Step	Laser output (mJ)	$^{40}Ar/^{39}Ar$	$^{37}Ar_{Ca}/^{39}Ar_K$ ($\times10^{-3}$)	$^{36}Ar/^{39}Ar$ ($\times10^{-3}$)	K/Ca	40Ar* (%)	39ArK (%)	$^{40}Ar^*/^{39}Ar_K$	Age (±1 sigma) (Ma)
Sample Eb-2, phlogopite megacryst			J=0.00202±0.4 %	Experiment number C07256		GeNF			
1	0.9	104.244 ± 0.573	0.327 ± 0.577	354.05 ± 3.69	1.8	0.0	1.1	0.029 ± 0.969	0.10 ± 3.54
2	1.0	23.888 ± 0.080	0.031 ± 0.159	78.59 ± 0.62	19.1	2.8	3.0	0.668 ± 0.173	2.44 ± 0.63
3	1.1	6.017 ± 0.023	0.012 ± 0.150	20.06 ± 0.37	48.9	1.5	4.5	0.090 ± 0.110	0.33 ± 0.40
4	1.2	4.646 ± 0.026	0.012 ± 0.061	14.82 ± 0.24	51.1	5.8	7.9	0.267 ± 0.072	0.98 ± 0.26
5	1.3	2.340 ± 0.011	0.032 ± 0.038	7.27 ± 0.10	18.3	8.3	13.1	0.195 ± 0.030	0.71 ± 0.11
6	1.4	2.112 ± 0.012	0.009 ± 0.044	6.46 ± 0.11	66.3	9.6	11.7	0.203 ± 0.033	0.74 ± 0.12
7	1.5	2.156 ± 0.013	0.014 ± 0.041	6.80 ± 0.12	43.2	6.9	11.8	0.149 ± 0.037	0.54 ± 0.13
8	1.6	1.017 ± 0.006	0.031 ± 0.077	3.03 ± 0.22	18.8	12.3	8.6	0.126 ± 0.065	0.46 ± 0.24
9	1.7	0.606 ± 0.005	0.009 ± 0.043	1.56 ± 0.16	62.7	24.3	9.8	0.147 ± 0.048	0.54 ± 0.18
10	1.8	1.149 ± 0.005	0.006 ± 0.040	3.34 ± 0.13	96.8	14.1	15.1	0.162 ± 0.039	0.59 ± 0.14
11	1.9	0.434 ± 0.004	0.029 ± 0.038	1.08 ± 0.16	20.4	27.4	12.8	0.119 ± 0.048	0.43 ± 0.18
12	4.0 (t.f.)	2.205 ± 0.035	0.141 ± 0.438	5.73 ± 2.72	4.2	24.0	0.7	0.530 ± 0.807	1.93 ± 2.94
Total gas age: 0.659±0.072 Ma			Plateau age: 0.631±0.053 Ma (gas fractions 4–11)		Isotope correlation age: 0.43±0.11 Ma			Inverse isotope correlation age: 0.43±0.11 Ma	
Sample Eb-1, amphibole megacryst			J=0.00205±0.4 %	Experiment number C07258		GeNF			
1	1.4	182.220 ± 4.443	4.719 ± 7.187	614.83 ± 27.04	0.1	0.6	0.0	1.131 ± 6.754	4.18 ± 24.93
2	1.5	10.204 ± 0.276	4.655 ± 4.823	21.76 ± 11.48	0.1	42.7	0.0	4.374 ± 3.458	16.11 ± 12.68
3	1.6	8.768 ± 0.464	2.160 ± 0.578	30.04 ± 2.77	0.3	1.8	0.2	0.160 ± 0.785	0.59 ± 2.90
4	1.7	4.308 ± 0.018	1.977 ± 0.243	14.52 ± 0.86	0.3	6.1	0.5	0.264 ± 0.258	0.98 ± 0.95
5	1.8	1.758 ± 0.007	1.980 ± 0.136	5.94 ± 0.30	0.3	14.2	1.1	0.251 ± 0.092	0.93 ± 0.34
6	1.9	1.505 ± 0.008	1.991 ± 0.063	4.64 ± 0.13	0.3	25.4	2.2	0.383 ± 0.039	1.42 ± 0.14
7	2.0	1.130 ± 0.005	2.133 ± 0.056	3.38 ± 0.09	0.3	35.2	3.7	0.398 ± 0.027	1.47 ± 0.10
8	2.1	0.841 ± 0.004	2.076 ± 0.055	2.37 ± 0.10	0.3	47.4	4.0	0.399 ± 0.030	1.48 ± 0.11
9	2.2	0.803 ± 0.003	2.094 ± 0.039	2.19 ± 0.04	0.3	51.9	5.5	0.417 ± 0.014	1.54 ± 0.05
10	2.3	0.724 ± 0.003	2.121 ± 0.035	2.06 ± 0.03	0.3	52.7	6.0	0.382 ± 0.009	1.41 ± 0.04
11	2.4	0.877 ± 0.004	2.106 ± 0.034	2.42 ± 0.04	0.3	48.6	6.3	0.427 ± 0.014	1.58 ± 0.05
12	2.5	0.820 ± 0.003	2.118 ± 0.029	2.08 ± 0.05	0.3	57.1	7.4	0.470 ± 0.016	1.74 ± 0.06
13	2.6	0.671 ± 0.002	2.127 ± 0.041	1.74 ± 0.04	0.3	62.7	5.9	0.422 ± 0.014	1.56 ± 0.05
14	3.3	0.730 ± 0.003	2.062 ± 0.025	1.75 ± 0.02	0.3	64.4	8.9	0.471 ± 0.008	1.74 ± 0.03
15	4.0 (t.f.)	0.877 ± 0.003	2.081 ± 0.010	2.44 ± 0.01	0.3	47.3	48.3	0.416 ± 0.004	1.54 ± 0.02
Total gas age: 1.553±0.016 Ma			Plateau age: 1.526±0.020 Ma (gas fractions 7–13)		Isotope correlation age: 1.40±0.09 Ma			Inverse isotope correlation age: 1.42±0.08 Ma	